MIT Libraries | DSpace@MIT

MIT Open Access Articles

A custom-designed limited-angle actuator for an electromechanical engine valve drive Part II: Fabrication and evaluation

Massachusetts Institute of Technology

A CUSTOM-DESIGNED LIMITED-ANGLE ACTUATOR FOR AN ELECTROMECHANICAL ENGINE VALVE DRIVE PART II: FABRICATION AND EVALUATION

Yihui Qiu, David J. Perreault, John G. Kassakian, Thomas A. Keim

Laboratory for Electromagnetic and Electronic Systems, Massachusetts Institute of Technology, MA, USA
Email: qiu@alum.mit.edu

Abstract

Research has shown that variable valve timing (VVT) can improve significantly the performance of internal combustion (IC) engines, including higher fuel efficiencies, lower emissions, and larger torque outputs at each point of the engine map. To achieve independent and continuous VVT for each valve, an electromechanical valve drive (EMV) system with a custom-designed limited-angle actuator was proposed previously, whose feasibility with lower power consumption, smaller package, and faster transition was predicted by simulation. In order to validate the concept experimentally, a prototype actuator was built and evaluated in this paper. The fabrication considerations and assembling process of the prototype actuator are discussed before satisfactory experimental results of the whole EMV system with the prototype actuator are presented. A further projection for a full engine valve actuation illustrates a promising future of the EMV system with the limited-angle actuator in a real engine environment up to an engine speed of 6000 rpm.

1 Introduction

Despite the simple design and low cost of the conventional crankshaft-synchronized cam driven valve actuator, it can offer optimized engine performance at only one point on the engine torque-speed operating map, commonly at the high load and high speed condition. On the other hand, VVT can offer optimal engine performance with significantly improved fuel economy, emissions and torque under any operating condition [1]-[7].

Based on the study of previous work of variable valve actuation (VVA), such as pure mechanical systems [6], [8], [12], an electro-hydraulic system [1], and electromechanical systems [4], [9]-[16], a novel EMV system using a shear force actuator was proposed several years ago [17]. Feasibility of the concept has been validated and performance enhancements have been achieved by previous work [18]-[20]. However, a much smaller actuator is needed to fit into the limited space over the engine head. A custom-designed

limited-angle actuator turns out to be a promising solution to this challenge.

Section 2 reviews the conceptual design of the proposed limited-angle actuator with its background and motivation. Section 3 presents fabrication considerations and assembling process of the prototype actuator. Experimental results of the whole EMV system with the prototype actuator are addressed in Section 4. Section 5 concludes the paper.

2 The proposed limited-angle actuator

In conventional IC engines, the valves are actuated by cams that are located on a belt- or chain-driven camshaft. As a long developed valve drive, the system has a simple structure, low cost, and offers smooth valve motion. However, the valve timing of the traditional valvetrain is fixed with respect to the crankshaft angle because the position profile of the valve is determined purely by the shape of the cam. If instead the valve timing can be decoupled from the crankshaft angle and can be adjusted adaptively for different situations, then the engine performance can be optimized with respect to higher torque/power output at any point of the engine map, achieving a fuel economy improvement of 5~20%, a torque improvement of 5~13%, an emission reduction of 5 ~10% in HC, and 40~60% in NO_x [1]-[7]. This flexibly controlled valve timing is called variable valve timing (VVT) and the corresponding valve drive system is called variable valve actuation (VVA).

The concept of electromechanical actuation has become feasible and attractive recently owing to its simple structure, continuous VVT control, and independent action for each valve and each cylinder. The Pischinger EMV system and close variants on that concept have become a popular research topic and has come closest to achieving commercial application [9]-[15].

To solve the landing problem, a new type of electromechanical valve drive has been proposed [17]. This EMV system inherits the valve-spring system and its regenerative benefits from the Pischinger EMV system, while using a bi-directional shear force actuator with a uniform torque constant. As shown in Fig. 1, the motor shaft is connected to the valve-spring system via a nonlinear mechanical transformer (NMT). The NMT is implemented by

a slotted cam and a roller follower in the slot which are connected to the motor shaft and the valve stem respectively. When the motor swings back and forth within the angle range limited by the cam slot design, the roller follower moves back and forth within the slotted cam, allowing the valve to move up and down between fully open and fully closed positions. In order to achieve soft landing at the end of transitions, low torque requirement during transitions, and zero power consumption between transitions, the mechanical transformer was designed with an intentionally nonlinear characteristics, as discussed in previous papers [17]-[22].
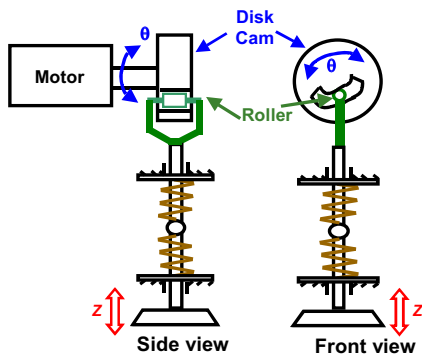

Fig. 1. The proposed EMV system.

Two commercial motors were used to validate the proposed EMV system, as shown in Fig. 2. A permanent magnet dc motor (the 4N63-100 from Pacific Scientific, Rockford, IL), was picked for our first prototype because it has a very high torque-to-rotor inertia ratio. However, this motor is too large to fit into the limited space over the engine head, especially if independent control for each valve is wanted in order to maximize the benefits. Therefore a brushless dc motor (Portescap B1118-050A), which has a much smaller size (about one seventh that of the old dc brush motor), was picked for our second try. This brushless motor is satisfactory in term of size, but its efficiency is too low and its ohmic loss and hence total power consumption is too high [21]. This suggested that a conventional motor design was probably not the best choice for the valve actuation application and motivated a custom-designed actuator, taking advantage of the application's special feature as of limited angle rotation. The customized actuator will offer small physical dimensions, low power consumption, as well as fast valve actuation.
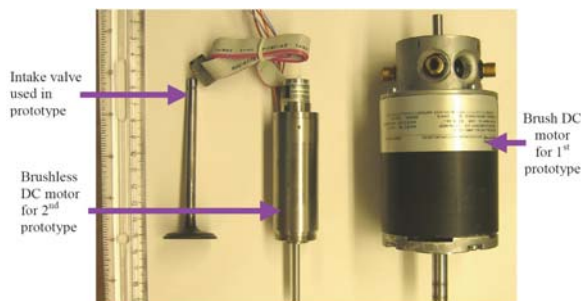

Fig. 2. The valve, the brush dc motor, and the brushless dc motor.

2.1 The proposed limited-angle actuator

In this application, the rotor only needs to swing back and forth within a limited angle range, which allows us to design a yoke structure and hence flux path that could not be used in a conventional motor. The cross section view of proposed limited-angle actuator is shown in Fig. 3. As discussed thoroughly in [21], the EMV system simulation with the custom designed actuator predicts a fast transition with reasonable power consumption. In a SolidWorks® design, as shown in Fig. 4, it clearly demonstrates the possibility of realizing independent valve actuation for a regular 4-cylinder 16-valve IC engine using our EMV system with the custom designed limited-angle actuator [21].
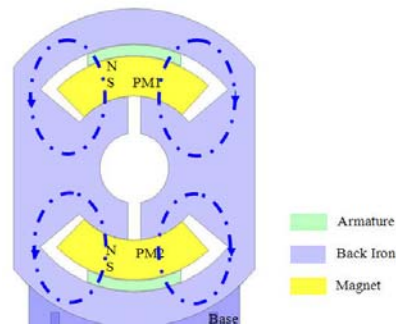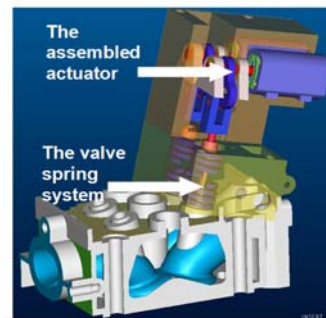

Fig. 3. Topology of the limited-angle actuator.

Fig. 4. Independent valve actuation system mounted on an engine head.
(courtesy to ITRI)

3 Building the prototype actuator

This section will focus on how to transfer the conceptual design into a detailed practical design. We will start with the hollow rotor winding fabrication. Then we will discuss material choices and design considerations of other components, including the iron yoke, permanent magnets, magnet spacers, bearings, shaft, and so on. Finally, we will illustrate how to assemble the actuator step by step.

3.1 Armature

The conceptual design discussed in a companion paper established design parameters such as thickness and the angle range of the armature. Here we determine the number of turns, what kind of insulation we will use, and how to construct the winding and with what materials.

Based on simulation, we designed a 4-turn winding for a 12 V bus. Each turn is designed as an aluminium rectangular conductor with a height of 1.3 mm and a width of 2.3 mm. We will strive to insure that insulation will have a thickness of 0.1 mm or less at each side to satisfy the 1.5 mm thickness and 45° angular range in the conceptual design.

Because we leave an air gap of only 0.2 mm between each side of the armature and the stator, we need the winding dimensions to be very accurate. Therefore, we built a mold for making the armature. The mold consists of 7 parts, as labelled in Fig. 5. The first three parts (mold 1-3) form a cylinder whose diameter is the same as that of the inner diameter of the armature. Mold parts 4 and 5 are two identical arc portions of a hollow cylinder, which have the same inner and outer diameters as the armature. Mold parts 1 to 5 can be screwed together to create a fixture. Mold parts 6 and 7 again are two identical arc portions of a hollow cylinder, which have an inner diameter the same as the outer diameter of the armature. These two parts will be clamped over parts 4 and 5, as shown in Fig. 5. The two air spaces between these parts define the exact shape of the active portions of the armature.

We also need to connect the armature and shaft together to form the rotor of the actuator. First, we designed two parts called the front-end clamp and back-end clamp. The end turns of the armature are placed between the two clamps and screws are used to clamp the two parts and the end turns together. Finally we connect the front-end clamps to the shaft via spring pins. The structure is shown in Fig. 6.
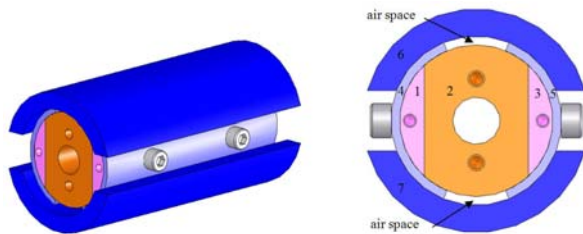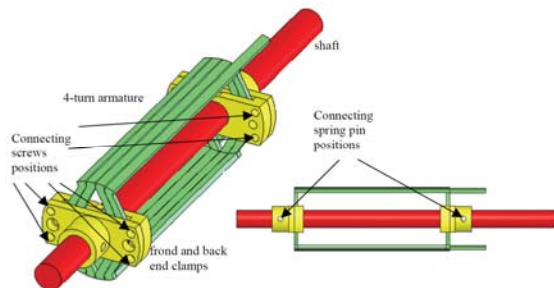

Fig. 5. Mold to make the armature.

Fig. 6. Armature-shaft structure.

Next we will discuss how to achieve a properly insulated and strong enough armature structure by taking advantage of epoxy pre-impregnated fiberglass tape and fiberglass woven sleeve. There are several wave patterns potentially suitable for this application, as discussed in [21]. The pattern we chose for the prototype is shown in Fig. 7.
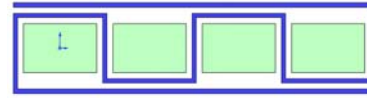

Fig. 7. Insulation pattern 1.

After the winding process, the end turns of the winding need to be pushed into the air space between the two end clamps in a way such that there is enough space between turns for the shaft, as shown in Fig. 6. Therefore the same woveing technique cannot be applied to the end turns because after winding, the positions of the end turns will be changed dramatically to fit into the end clamps and to allow the shaft to pass through, requiring the end turns to be insulated separately. A fiberglass woven sleeve is chosen to fulfil this purpose. For mechanical reasons, epoxy resin is dropped onto the sleeved end turns to ensure strong connections between all end turns and between the end turns and the clamps.

The step-by-step building process of the winding structure is illustrated in [21]. The finished armature as well as the armature model in Solidworks® is shown in Fig. 8.
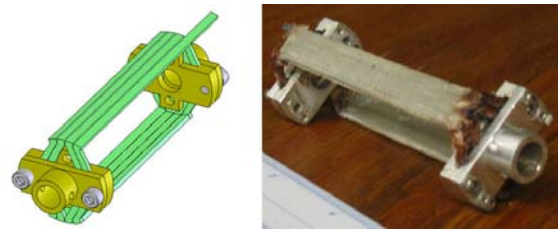

Fig. 8. SolidWorks® model and the cured armature structure w/o shaft.

3.2 Other parts

A. Iron Yoke

Considering only its own function, we could make the yoke a single piece of mild steel. However, we need to install the armature and the permanent magnets within it, so as a practical matter, we chose to build it in multiple pieces. There are many possible approaches to do this, depending on the procedure to be used to assemble the whole actuator. Here we choose to build the iron yoke from three layers and five pieces, as shown in Fig. 9, with screws in the sides to hold them together. We will refer to the three layers from outside to inside as core 1, core 2, and core 3, respectively.
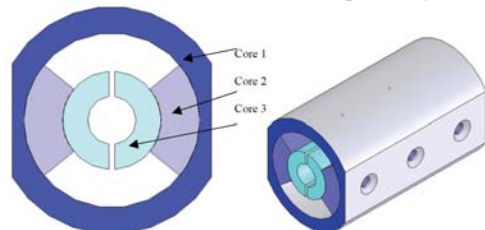

Fig. 9. Three-layer and five-piece design of the iron yoke.

B. Shaft and Bearings

Since the armature is the only moving element of the actuator, it is preferred to use a shaft with a large diameter to increase the ruggedness of the armature-shaft structure. For our design,

the diameter of the shaft is 5/16 in, very close to that of the first motor (3/8 in) and much larger than that of the second motor (3/16 in). The shaft is made from a stainless steel rod with a tight dimensional tolerance and a precision ground finish (Mcmaster 8934K23).

Ball bearings support the shaft at both ends in order to minimize friction. To avoid a complicated and bulky bearing housing outside of the actuator, the ball bearings are press fit into the inner layer of the iron yoke. Hence, we need to modify core 3 with a properly sized cavity at both ends to accommodate the ball bearings, as shown in Fig. 10, where the bearings are represented by a pink hollow cylinder. A Maxwell® simulation has been done to ensure that no calculated reduction of torque output is expected due to this modification of core 3. The stainless steel ball bearing (Mcmaster 57155K358), has an inner diameter (ID) of 5/16 in, an outer diameter (OD) of 1/4 in, and a width of 5/32 in.
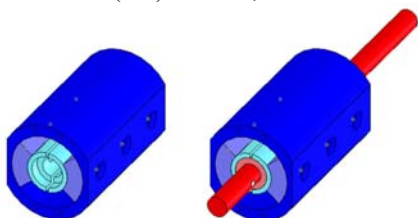

Fig. 10. Modified core 3 to accommodate ball bearing to support shaft.

C. Permanent Magnets and Magnet Spacers

The high temperature grade Neodymium-Iron-Boron (NdFeB) permanent magnets (NingBo Zhaobao Magnet Co, LTD, China) are used for high flux excitation. The magnets are specified as an arc section of a hollow cylinder, which has an ID of 16.4 mm, an OD of 25.4 mm, hence a radial thickness of 4.5 mm, and an arc range of 90°.

To prevent the magnets from moving axially or rotating with respect to the axis during or after the actuator is assembled, aluminium magnet spacers are used to hold them in desired positions during and after the assembling procedure. The spacers are fixed to the inner layer of the iron yoke via screws, as shown in Fig. 11, where the spacers are represented in gray and the magnets are shown in yellow.
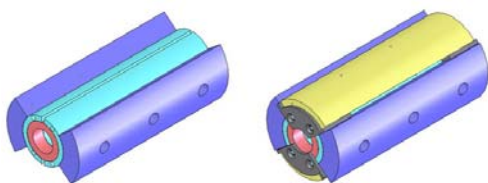

Fig. 11. Permanent magnets and magnet spacers.

D. Encoder and Mounting Bridge

Because we need θ position feedback to monitor and control the transition trajectory, a micro hollow shaft optical encoder (2MCH from Scancon Incremental Encoders, USA) is used. This encoder can only accommodate a shaft with a diameter of no more than 1/8 inch. The encoder is designed to be installed using a mounting plate included in the encoder

package. A mounting bridge is used to connect the stationary mounting plate of the encoder to the stationary part of the actuator --- the outside layer of the iron yoke. Further, we need to reduce the encoder end of the shaft to a diameter of 1/8 inch to fit the rotating part of the encoder. Fig. 12 shows more details about this design consideration.
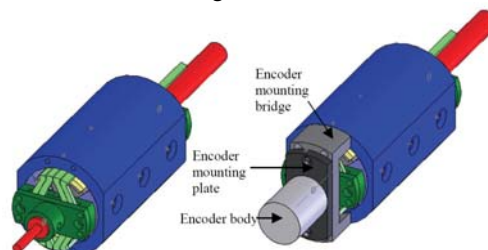

Fig. 12. Shaft and core 1 modification for encoder installation.

3.4 Assembling the Actuator

In this subsection we discuss how to assemble all the parts to obtain a functional actuator. We start assembling by attaching the two pieces of core 3 and the two pairs of magnet spacers together, as shown in Fig. 13. Two slim plastic spacers with a thickness of 1mm and proper height and length are inserted into the air gaps between the two pieces of core 3 before assembling. Then the two ball bearings shown in pink are pressed into the core. A pair of permanent magnets is then put into the positions defined by the magnet spacers, as also shown in Fig. 13.
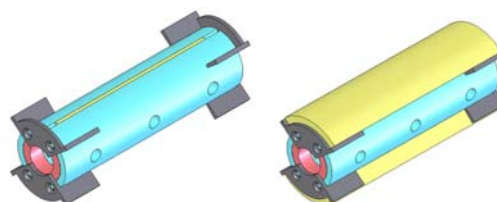

Fig. 13. Assembling of core 3, core spacers, magnet spacers, and PMs.

The rotor, i.e., the armature-shaft structure, is installed next. At this point the shaft is not fixed to the front end clamps. As shown in Fig. 13, the armature is placed on top of the partial assembly. The orientation of the armature will allow it to slide over the partial stator assembly. The shaft, which goes through the end clamps of the armature and the clearance hole within core 3, is then installed. The armature is next rotated 90° with respect to the partial stator assembly so that it is positioned with the active turns centered on the permanent magnets. Spring pins are then used to permanently connect the rotor shaft and end clamps.

After fitting the armature into the partial stator assembly, we are ready to put on the second layer of the iron yoke by putting the two pieces of core 2 into the positions defined by the magnet spacers and the two pieces of core 3, as shown in Fig. 15. The outside layer of the iron yoke (core 1) is now slid on from either end and connected to core 2, and core 3 by flat-head screws, as also shown in Fig. 15.
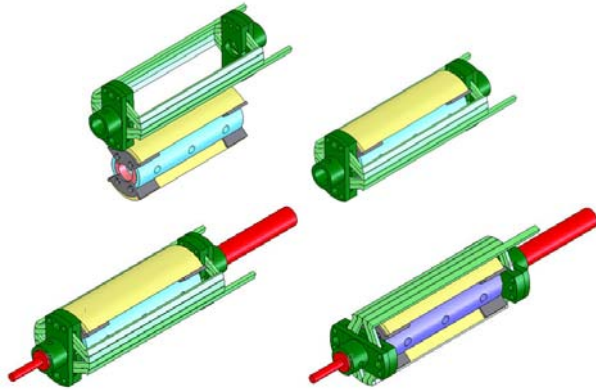
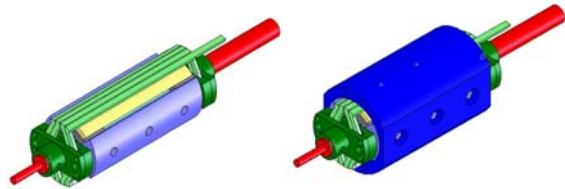Fig. 14. The four steps of assembling the armature and partial core.

Fig. 15. Cores 3, 2, and 1 added to complete the stator assembling.

Finally, we installed the encoder and its accessories in the following sequence. First, the mounting bridge is connected to the core 1 by screws; then, the mounting plate is connected to the mounting bridge also by screws; and lastly, the rotating part of the encoder is connected to the shaft by a set screw and the stationary part of the encoder is fixed to the mounting place by a flat spring. This process is shown in Fig. 16. Note that the set screw and flat spring in the last step are not shown in Fig. 16.
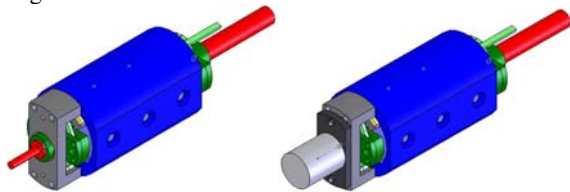

Fig. 16. The encoder installed on the actuator.

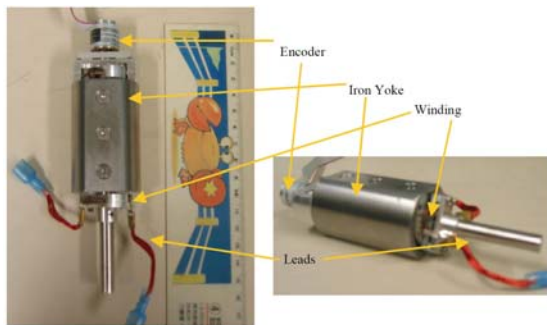The picture of the assembled actuator is shown in Fig. 17.

Fig. 17. The fully assembled limited-angle actuator.

4 Experimental Validation

Before installed into the actuator, the armature was tested in physical dimensions, mechanical strength, and electrical parameters (resistance and inductance). After the prototype actuator was fully assembled, we also did some testing to make sure the actuator has the desired torque constant, rotor inertia, and friction coefficients. All testing results show good matching with our expectations, as discussed thoroughly in [21] and selectively summarized in Table I.

Table I: The measurements summary of the actuator.

	Expected Value	Tested Value
Torque constant (mN-m/A)	5.09	5.22
Armature R (mOhm)	7.7	8.0
Armature L (uH)	4.8	5.0
Rotor&cam inertia (Kg·m²/s)	$1.47 \cdot 10^{-5}$	$1.8 \cdot 10^{-5}$
Rotor friction coefficient (μN-m·s/rad)	500	500
Valve friction coefficient (N-m/s)	12	6

The full experimental setup is shown in Fig. 18. Note that the armature of the actuator is directly connected to the outside drive via two stranded wires for simplicity. For a more practical design, some alternative device, such as a pair of elastic spring leads, can be used to connect the rotating armature and outside power supply. Also note that between the drive and the actuator, there is an extra inductor inserted for the purpose of maintaining an appropriate switching frequency due to the limitation of the drive [21].
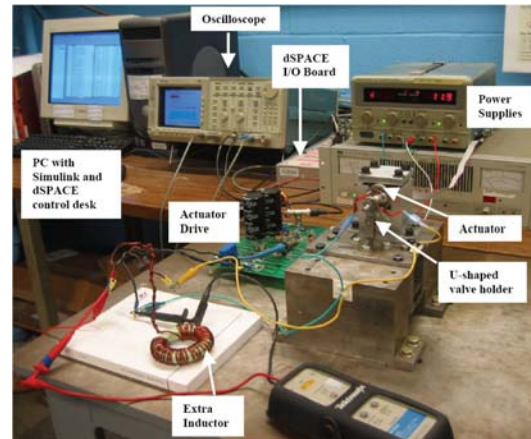

Fig. 18. The experimental setup with the limited-angle actuator.

Following the optimized control strategy discussed in [21][22], we use a single current pulse to complete the valve actuation. Current pulses with different amplitudes and durations have been used and the resulting transition times and different amounts of power recorded. Two examples are presented in this paper. As shown in Fig. 19, one transition achieved using a 75 A, 6.5 ms current command and result in a transition time of 2.6 ms and power consumption of 49 W while another transition achieved with a 60 A, 9 ms current command and result in a transition time of 2.7 ms and power consumption of 44 W, as shown in Fig. 20.
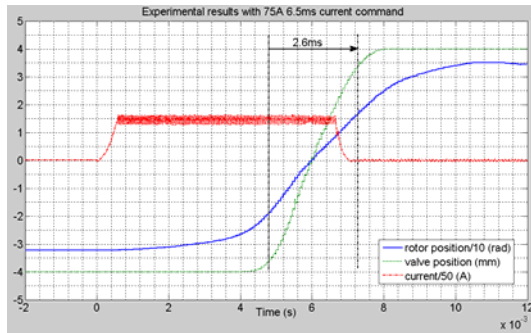
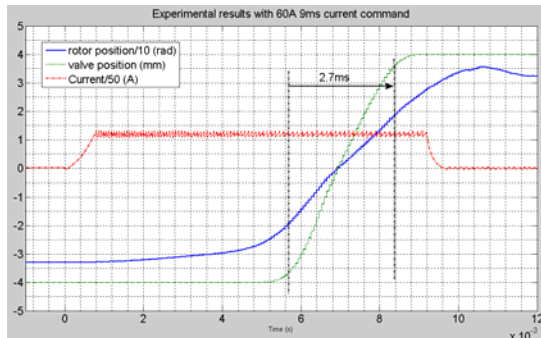Fig. 19. Experimental results with 75 A, 6.5 ms current command.

Fig. 20. Experimental results with 60 A, 9 ms current command.

Due to the limited experimental setup, we did not conduct experiments on opening of the exhaust valve against a large gas force. However, the simulation confirms that this actuator is capable of opening an exhaust valve with a transition time of 2.9 ms and a power consumption of 102 W. From the simulation with gas force and the experiment of valve actuation without gas force, we can project the performance of a full valve actuation system for a 4-cylinder 16-valve engine at 6000 rpm, as summarized in Table II below [21].

Table II: Performance projection of a full valve actuation system.

	Actuate intake valve w/o gas force	Close exhaust valve w/o gas force	Open exhaust valve w/ gas force
Transition time(ms)	2.6	2.6	2.9
Average power / half cycle (W)	49	49	102
Average power /cycle (W)	49	75.5	
Average power of a engine/cycle (W)	996		

5 Conclusions

This paper present the fabrication process and experimental validation of a custom-designed limited-angle actuator proposed previously for an electromechanical valve drive to provide VVT in IC engines with a small enough package (to fit in the limited space over the engine head), a fast enough transition time (to accommodate faster engine speed), and a low enough power consumption. The customized limited-angle actuator enabled the projection of independent valve actuation for a 4-cylinder 16-valve IC engine with reasonable power consumption and engine speed up to 6000 rpm.

Acknowledgements

References

[1] M. B. Levin, and M. M. Schlecter, "Camless Engine", *SAE Technical Paper Series*, Paper 960581, 1996.
[2] P. Barkan, et. al., "A Review of Variable Valve Timing Benefits and Modes of Operation," *SAE Technical Paper Series*, Paper 891676, 1989.
[3] T. Ahmad, et, al., "A Survey of Variable-Valve-Actuation Technology," *SAE Technical Paper Series*, Paper 891674, 1989.
[4] M. Pischinger, et. al., "Benefits of the Electromechanical Valve Train in Vehicle Operation," SAE Technical Paper Series, Paper 2001-01-1223, 2001.
[5] C. Tai, et. al., "Increasing Torque Output from a Turodiesel with Camless Valve Train," SAE Technical Paper Series, Paper 2002-01-1108, 2002.
[6] M. Sellnau, et. al., "Two-Step Variable Valve Actuation for Fuel Economy, Emissions, and Performance," SAE Technical Paper Series, Paper 2003-01-0029, 2003.
[7] G. B. Parvate-Patil, et. al., "An Assessment of Intake and Exhaust Philosophies for Variable Valve Timing," SAE Technical Paper Series, Paper 2003-32-0078, 2003.
[8] R. Steinberg, et. al., "A Fully Continuous Variable Cam Timing Concept for Intake and Exhaust Phasing", SAE Technical Paper Series, Paper 980767, 1998.
[9] F. Pischinger, et. al., "Electromechanically Operating Actuators," U.S. Patent 4,455,543, 1984.
[10] F. Pischinger, et. al., "Electromechanical Variable Valve Timing," Automotive Engineering International, 1999.
[11] M. Gottschalk, "Electromagnetic Valve Actuator Drives Variable Valvetrain," Design News, November 1993.
[12] R. Flierl, and M. Klüting, "The Third Generation of Valvetrains --- New Fully Variable Valvetrains for Throttle-Free Load Control," SAE Technical Paper Series, Paper 2000-01-1227, 2000.
[13] S. Butzmann, et. al., "Sensorless Control of Electromagnetic Actuators for Variable Valve Train," SAE Technical Paper Series, Paper 2000-01-1225, 2000.
[14] K. Peterson, et. al., "Nonlinear Self-tuning control of Soft Landing of an Electromechanical Actuator," Proc. 2nd IFAC Conference on Mechatronics Systems, Berkeley, CA, 2002.
[15] K. Peterson, et. al., "Rendering the electromechanical valve actuator globally asymptotically stable," Proc. 42nd IEEE Conference Decision and Control, Maui, HI, Dec. 2003, pp. 1753–1758.
[16] D. Durrieu, et. al., "Electro-Magnetic Valve Actuation System: First Steps Toward Mass Production," SAE Technical Paper Series, Paper 2008-01-1360, 2008.
[17] W. S. Chang, "An Electromechanical Valve Drive Incorporating a Nonlinear Mechanical Transformer," Ph.D. thesis, MIT, 2003.
[18] T. A. Parlikar, "Experimental Implementation of an Electromagnetic Engine Valve", Master Thesis, MIT, 2003.
[19] Y. H. Qiu, et. al., "Design and Experimental Evaluation of An Electromechanical Engine Valve Drive," in Proceedings of the 35th IEEE Power Electronics Specialists Conference, pp. 4838-4843, Aachen, Germany, June, 2004.
[20] T. A. Parlikar, et. al., "Design and Experimental Implementation of an Electromagnetic Engine Valve Drive", in IEEE/ASME Transaction on Mechatronics, Vol.10, NO.5, October 2005.
[21] Y. H. Qiu, "Advanced Modeling, Control, and Design of an Electromechanical Engine Valve Drive System with a Limited-angle Actuator," Ph.D. thesis, Massachusetts Institute of Technology, 2009.
[22] Y. H. Qiu, et. al., "Optimal Cam Design and System Control for an Electromechanical Engine Valve Drive", in proceedings of the.IEEE International Conference on Industrial Technology, 2010, accepted.